

## Supplementary Information

### Understanding the Interplay between Crystal Structure and Charge Transport in Alloyed Lead-free Perovskites

Aleksandra G.Boldyreva,<sup>a\*</sup>, Shijing Sun<sup>b</sup>, Polly J. Pierone<sup>c</sup>, Philipp Talalaev<sup>d</sup>, Janak Thapa<sup>b</sup>, Meng-ju Sher<sup>c</sup>, Noor Titan Putri Hartono<sup>b</sup>, Tonio Buonassisi<sup>b</sup>, Pavel A. Troshin<sup>d</sup>, and Keith J. Stevenson<sup>a</sup>

<sup>a</sup> Skolkovo Institute of Science and Technology Nobel street 3, Moscow, 143026, Russia

<sup>b</sup> Massachusetts Institute of Technology, Boston, Massachusetts, USA

<sup>c</sup> Wesleyan University, Middletown, Connecticut, USA

<sup>d</sup> Institute for Problems of Chemical Physics of the Russian Academy of Sciences (ICP RAS), Semenov prospect 1, Chernogolovka, 142432, Moscow region, Russia

\* Corresponding author: aleksandra.boldyreva@skolkovotech.ru

Table S1. Average P, R, D characteristics of the studied lateral devices (symbols in brackets show standard deviation). Bandgaps were estimated using Tauc plot, \* denotes for indirect bandgap.

Material	Dimansio nality	Bandgap (ass) eV	405 nm			532 nm			650 nm		
			P %	R mA/W	D Jones	P %	R mA/W	D Jones	P %	R mA/W	D Jones
MA <sub>3</sub> Bi <sub>2</sub> I <sub>9</sub>	0D	1.91*	51.4 (8.2)	2.8 (0.0925)	1.8·10 <sup>8</sup> (0.0925)	2.15 (48.8)	0.0041 (48.8)	2.4·10 <sup>5</sup> (48.8)	-	-	-
MA <sub>3</sub> (Bi <sub>0.6</sub> Sb <sub>0.4</sub> ) <sub>2</sub> I <sub>9</sub>	0D	1.89*	25 (8.2)	1.3 (0.0925)	8.4·10 <sup>7</sup> (0.0925)	3.9 (48.8)	0.0067 (48.8)	4.1·10 <sup>5</sup> (48.8)	-	-	-
MA <sub>3</sub> Sb <sub>2</sub> I <sub>9</sub>	0D	1.91*	314 (8.2)	19 (0.0925)	1.2·10 <sup>9</sup> (0.0925)	8.0 (48.8)	0.13 (48.8)	2.6·10 <sup>6</sup> (48.8)	4.6 (63.2)	0.4 (0.38)	7.4·10 <sup>6</sup> (0.38)
MA <sub>3</sub> Bi(I <sub>0.6</sub> Br <sub>0.4</sub> ) <sub>2</sub>	2D	2.25	3.6 (8.2)	0.16 (0.371)	1·10 <sup>7</sup> (0.371)	-	-	-	-	-	-
MA <sub>3</sub> (Bi <sub>0.6</sub> Sb <sub>0.4</sub> ) <sub>2</sub> (I <sub>0.6</sub> Br <sub>0.4</sub> ) <sub>2</sub>	2D	2.23	55.3 (8.2)	2.4 (0.371)	1.6·10 <sup>8</sup> (0.371)	6.8 (48.8)	0.012 (48.8)	7.3·10 <sup>5</sup> (48.8)	-	-	-
MA <sub>3</sub> Sb <sub>2</sub> (I <sub>0.6</sub> Br <sub>0.4</sub> ) <sub>2</sub>	2D	2.28	315 (8.2)	19 (0.0925)	1.2·10 <sup>9</sup> (0.0925)	8.9 (48.8)	0.016 (48.8)	1.0·10 <sup>6</sup> (48.8)	-	-	-
MA <sub>3</sub> BiBr <sub>9</sub>	2D	2.74	-	-	-	-	-	-	-	-	-
MA <sub>3</sub> (Bi <sub>0.6</sub> Sb <sub>0.4</sub> ) <sub>2</sub> Br <sub>9</sub>	2D	2.71	6.2 (8.2)	0.17 (0.371)	1.1·10 <sup>7</sup> (0.371)	-	-	-	-	-	-
MA <sub>3</sub> SbBr <sub>9</sub>	2D	2.75	58.9 (8.2)	4.2 (0.0925)	2.7·10 <sup>8</sup> (0.0925)	-	-	-	-	-	-

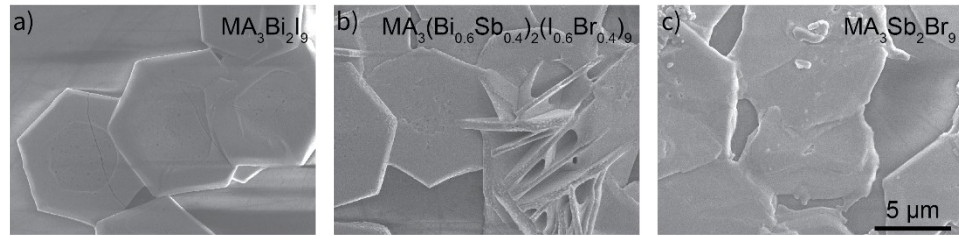


Figure S1. SEM images of 3 characteristic samples prepared on quartz showing micrometer size hexagonal grains and the resulting material exhibited the same carrier mobility but improved carrier lifetime.

Table S2. – THz measurements for 2 set of samples, prepared on quartz. (set #1 – bare perovskite solutions, #2– solutions with NH<sub>4</sub>SCN additive).

Sample Set #1	THz mobility, cm <sup>2</sup> /V/s	THz lifetime, ps
MA <sub>3</sub> Bi <sub>2</sub> Br <sub>9</sub> , (2D)	0.4	8.7
MA <sub>3</sub> Sb <sub>2</sub> Br <sub>9</sub> , (2D)	0.5	4.8
MA <sub>3</sub> (Bi <sub>0.6</sub> Sb <sub>0.4</sub> ) <sub>2</sub> (I <sub>0.6</sub> Br <sub>0.4</sub> ) <sub>9</sub> , (2D)	0.6	6.6
MA <sub>3</sub> Bi <sub>2</sub> I <sub>9</sub> (0D)	0.3	2.8
MA <sub>3</sub> Sb <sub>2</sub> I <sub>9</sub> , (0D)	0.4	1.2
Sample Set #2	THz mobility, cm <sup>2</sup> /V/s	THz lifetime, ps
MA <sub>3</sub> (Bi <sub>0.6</sub> Sb <sub>0.4</sub> ) <sub>2</sub> (I <sub>0.6</sub> Br <sub>0.4</sub> ) <sub>9</sub> , (2D)	0.4	12
MA <sub>3</sub> Sb <sub>2</sub> Br <sub>9</sub> , (2D)	0.4	10
MA <sub>3</sub> Bi <sub>2</sub> I <sub>9</sub> (0D)	0.3	9

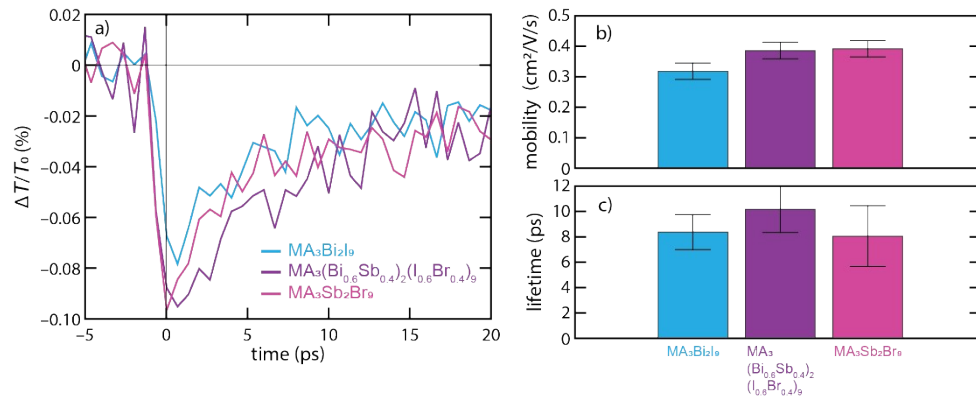


Figure S2. THz mobility and lifetime of samples prepared on quartz with the increased grain size, carrier lifetime increased to >9 ps for all samples while carrier mobilities remain the same.

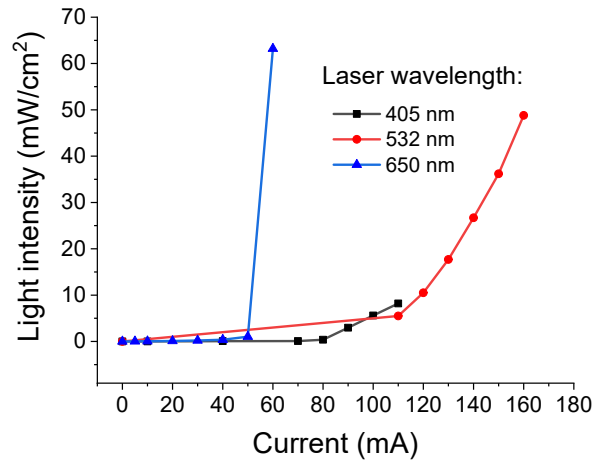


Figure S3. – Relation between laser light intensity and current

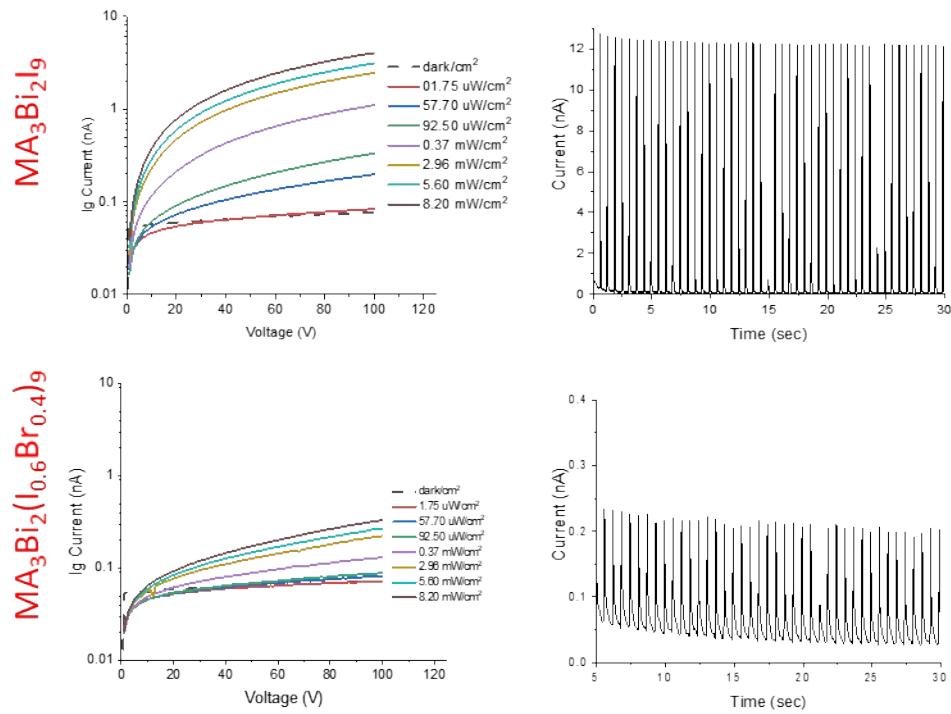


Figure S4. IV characteristics and transient photoresponse of Bi-systems ( $\text{MA}_3\text{Bi}_2\text{Br}_9$  did not respond)

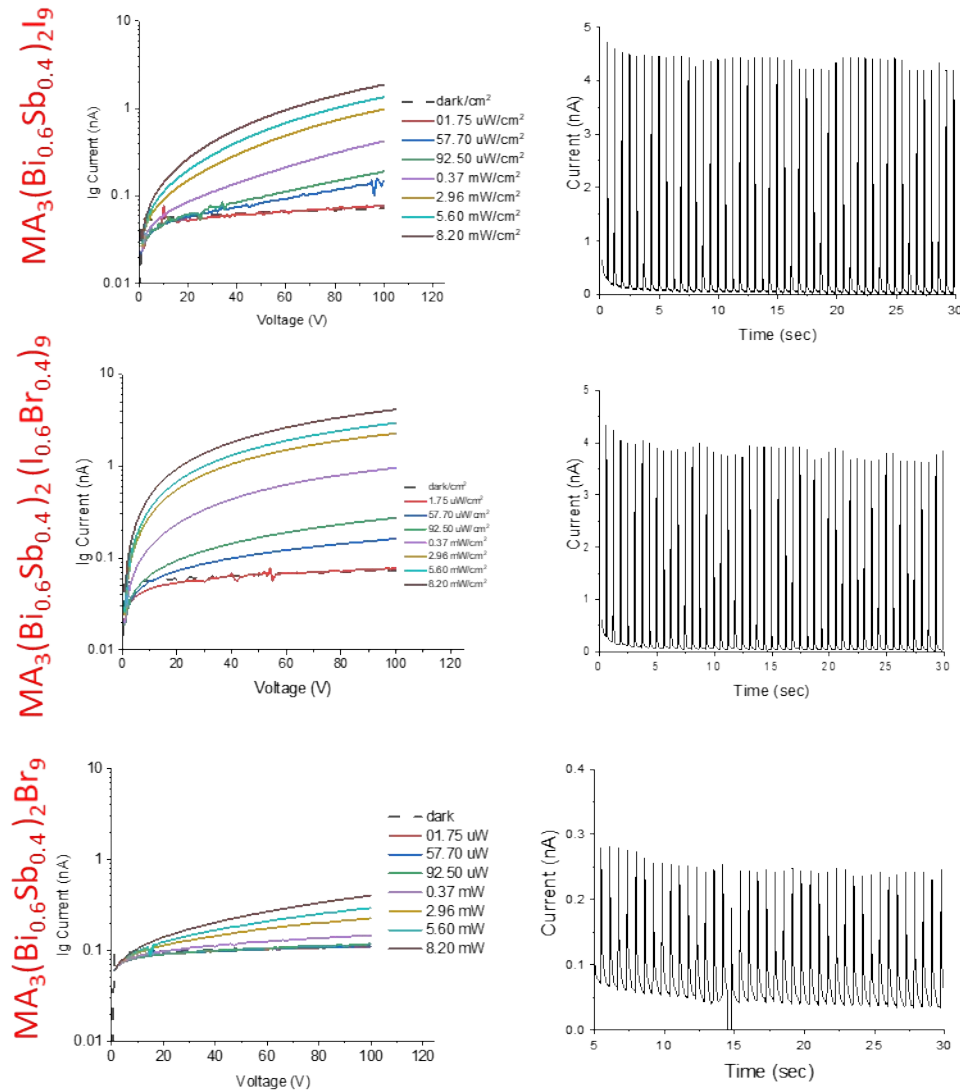


Figure S5. IV characteristics and transient photoresponse of Bi-Sb systems

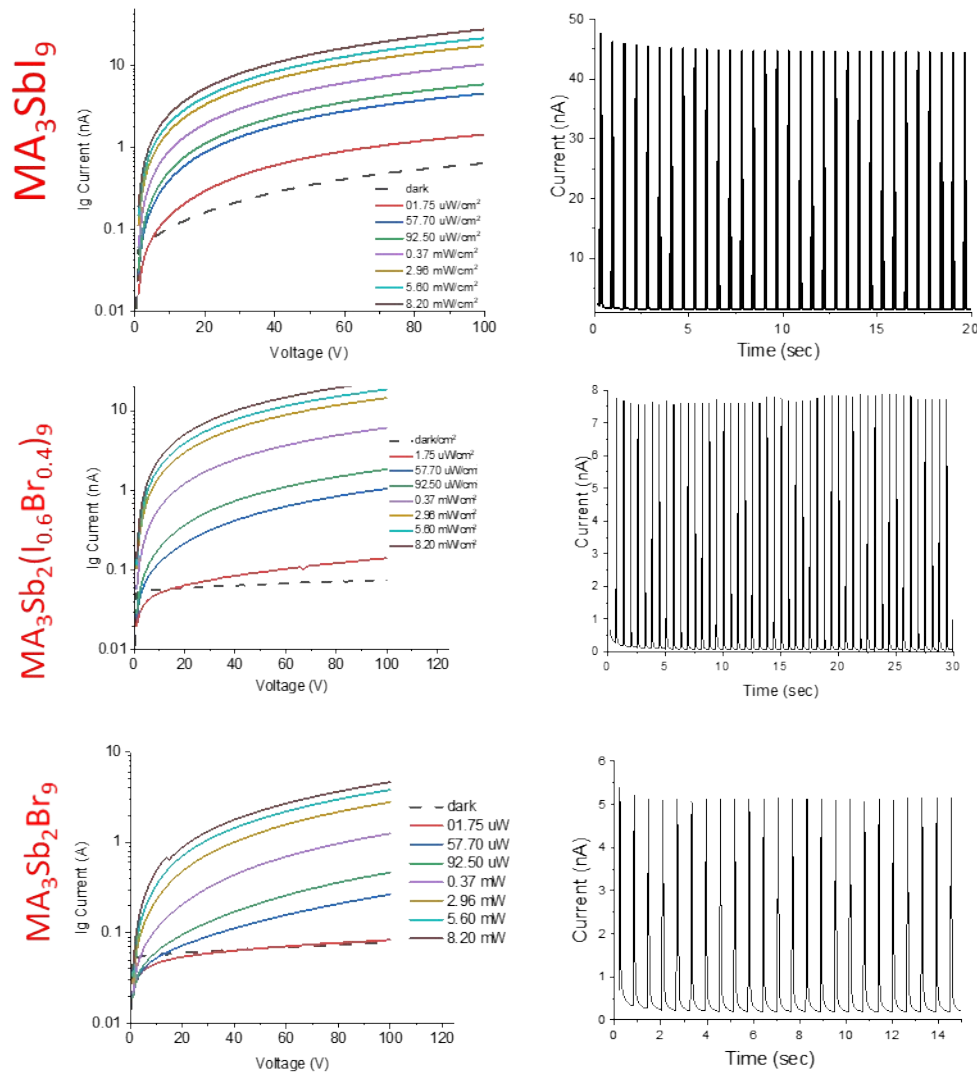


Figure S6. IV characteristics and transient photoresponse of Sb-systems

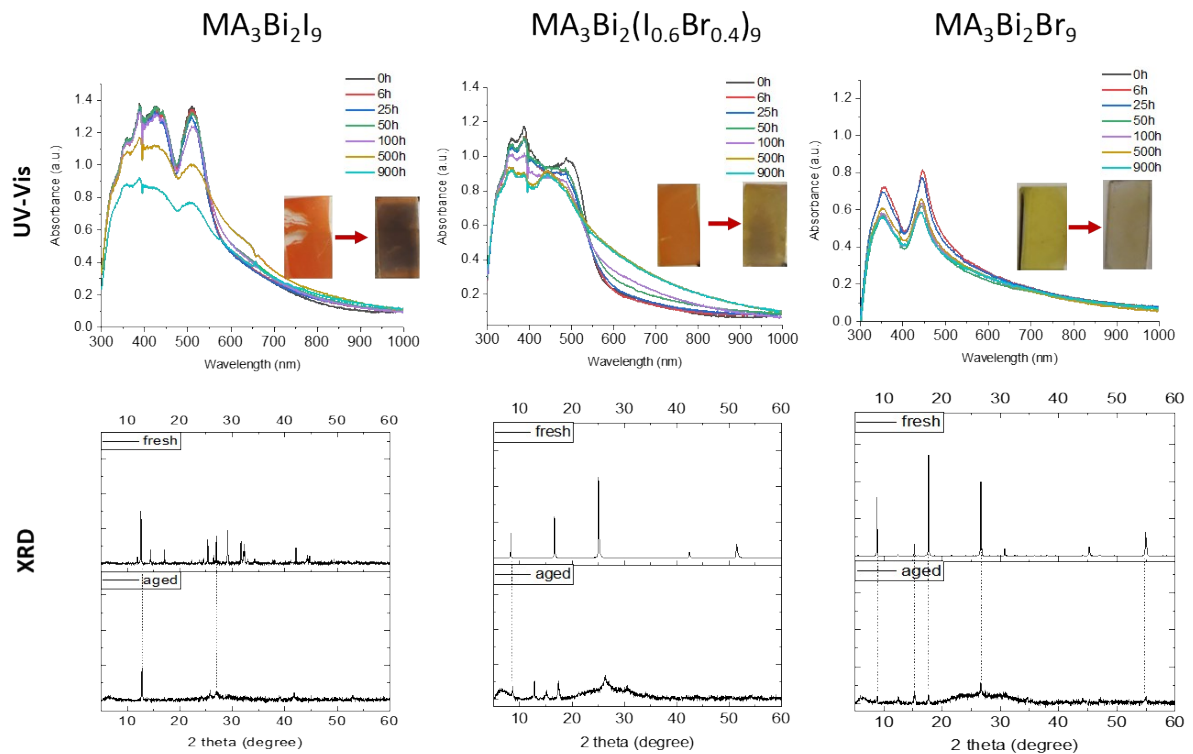


Figure S7. Change of UV-vis spectra(a) and XRD patern(b) of Bi-rich- systems.

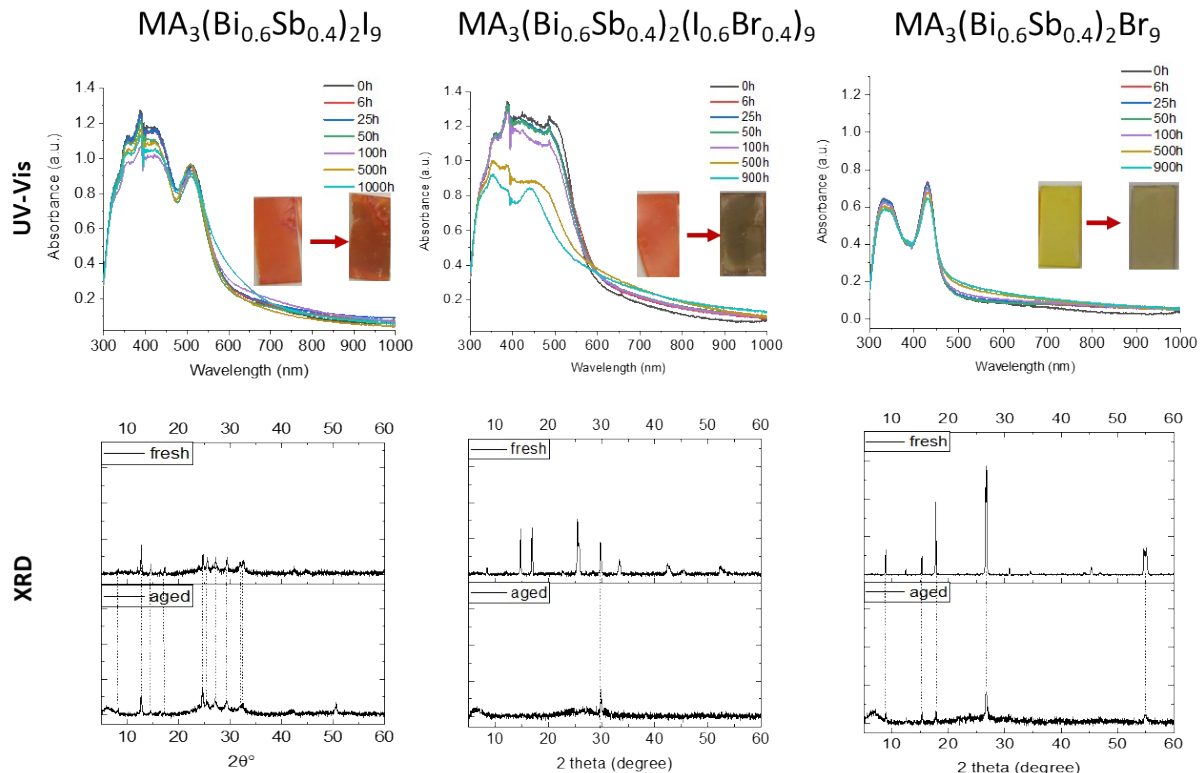


Figure S8. Change of UV-vis spectra(a) and XRD patern(b) Bi-Sb systems.

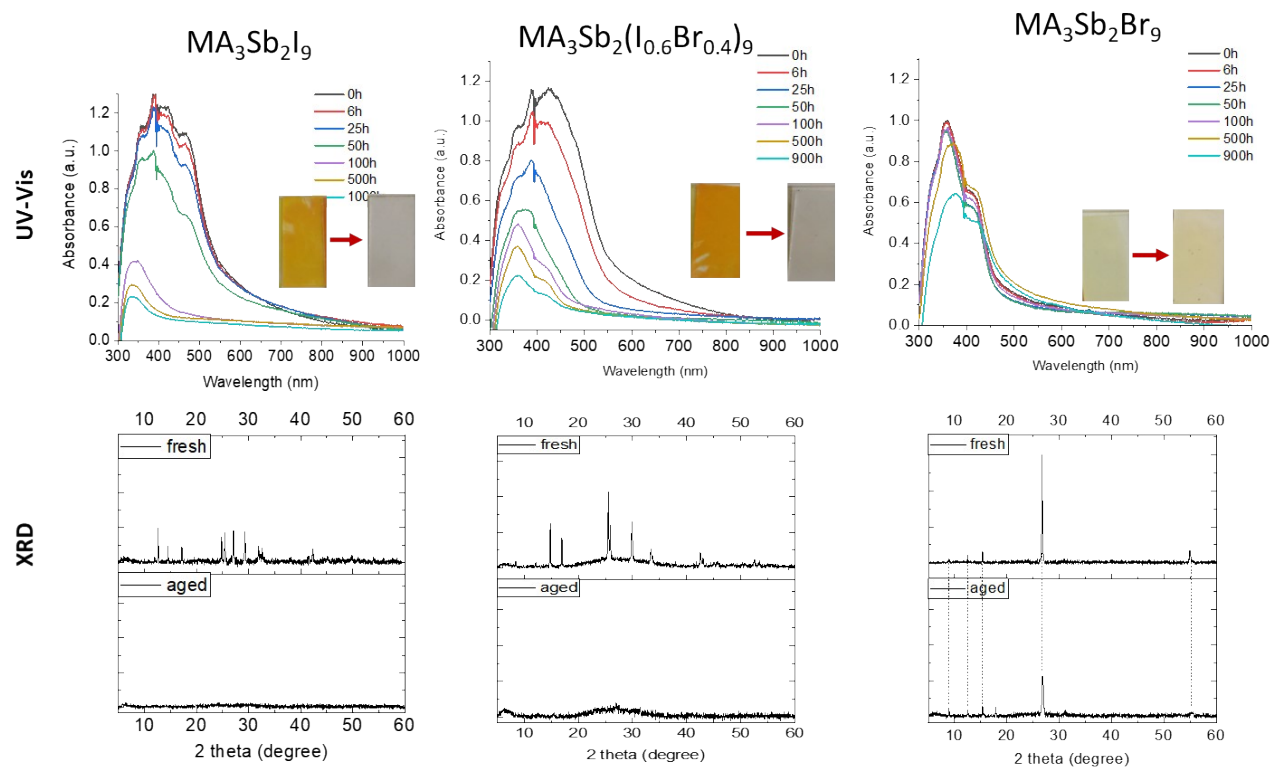


Figure S9. Change of UV-vis spectra(a) and XRD patern(b) of Sb-rich systems.